TWIST

Nano-Organometallic Compounds as Prospective Metal Based Anti-Lung Cancer Drugs:
Biochemical and Molecular Docking Studies

Abdou S. El-Tabl
Department of Chemistry, Faculty of Science, Menoufia University, Shebin El -Kom, Egypt

Sherif A. Kolkaila
Department of Chemistry, Faculty of Science, Damanhour University, Damanhour, Egypt

Shaymaa M. Abdullah
Department of Chemistry, Faculty of Science, Menoufia University, Shebin El -Kom, Egypt

Ahmed M. Ashour*
Department of Chemistry, Faculty of Science, Menoufia University, Shebin El -Kom, Egypt
[*Corresponding author]

Abstract
The great success of cis-platin as a chemotherapeutic agent considerably increased research efforts in inorganic biochemistry to identify more metallic drugs having the potential of treating lung cancer. Copper is a micronutrient essential to all organisms and is a critical impact in redox chemistry, growth and development. In biology copper has a crucial role for the function of several enzymes and proteins involved energy metabolism, respiration and DNA synthesis, notably cytochrome oxidase, super dismutase, ascorbate oxidase and tyrosinase. This study determined the selective cytotoxicity and mutagenic potential of two Schiff-base complexes nanoparticles of copper salts against lung cancer cell lines, "A549 cell lines" (*Invitro* study) and showed the toxicity action observed against experimental animals (*invivo* studies). The more effective and probable binding modes between the studied metal complexes NPs with different active sites of lung cancer (the selected protein 5HG5) receptors were investigated using molecular docking studies.

INTRODUCTION
Lung cancer is a malignant tumor that develops from the bronchial mucosa or glands of the lung, which poses the greatest threat to human health and lives, exhibiting the fastest increase rate in terms of morbidity and mortality [1]. In 2020, ~19.3 million new cancer cases and approximately 10 million cancer-related deaths were reported worldwide [2]. Lung cancer remains the leading cause of cancer-related death, engendering an estimated 1.8 million deaths (18%) with an estimated 2.2 million new cases (11.4%) in 2020 [3]. The dramatic increase in the cases of lung cancer and multidrug-resistant infections has necessitated the search for novel treatment options and strategies [4]. New small-molecule anti-cancer agents exhibit great potentials. However, the frequent occurrence of multidrug resistance (MDR) in lung cancer warrants the development of specific agents that can overcome MDR [5]. Metal-based drugs are structurally stable and have unique three-dimensional configurations, which can be effectively used to treat multidrug-resistant infections [6]. It was Barnett Rosenberg in 1965 that accidentally discovered the biological activity of cis-platin, which was recognized as an anticancer drug. The therapeutic activity of cis-platin is achieved by binding with DNA to form crosslinks as major lesions, thus inhibits replication and transcription processes and finally the cell's repair mechanism and leads to cellular apoptosis [7, 8]. Despite of good clinical success of cis-platin, it lacks tumor tissue selectivity leading to some severe side effects. Advances in nanotechnology and growing needs in biomedical applications have driven the development of

multifunctional nanoparticles [9]. Nanoparticles have the potential to be ideal carriers for delivering anticancer and other therapeutics to diseased sites with minimal collateral damage to normal tissues [10]. Functional copper nanoparticles (Cu NPs) have evoked keen interest in recent decades owing to their size- and shape-dependent optical, catalytic, and therapeutic properties. copper-based nanomaterial have been notable for excellent therapeutic applications. Functional Cu NPs have shown apoptosis-inducing properties through target specific pathways [11, 12]. This study aimed to evaluate the antitumor activity of Cu complex NPs against lung cancer cell lines using advanced biochemical methods.
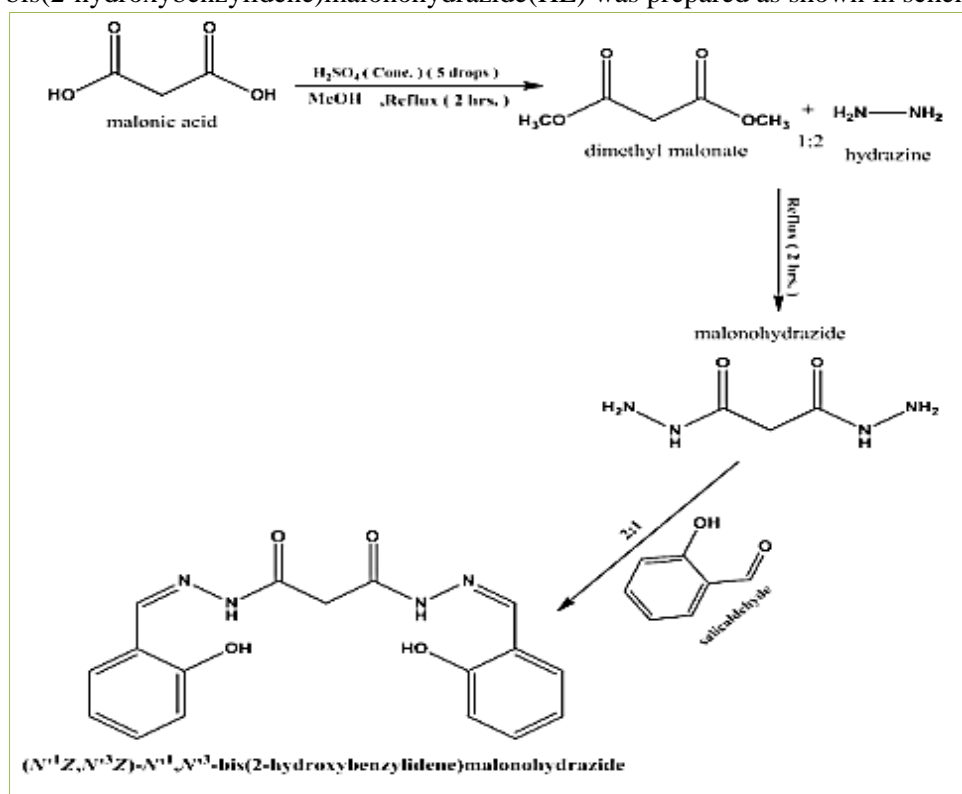
EXPERIMENTAL
Chemistry (Synthesis of complexes 1 & 2)
All solvents and reagents were of analytical grade and used without further purification.

Synthesis of the ligand
(N'^1E,N'^3E)-N'^1,N'^3-bis(2-hydroxybenzylidene)malonohydrazide(HL) was prepared as shown in scheme 1.

Scheme 1 Preparation of the ligand

Synthesis of the complexes
The metal complexes **(1&2)** were prepared by refluxing with continuous stirring of a suitable amount of a hot ethanolic solution of the metal salts, $Cu(OAc)_2(H_2O)$ & $CuSO_4.5H_2O$, respectively and then added to hot ethanolic solution of the ligand with a molar ratio (2 metal: 1 ligand) for 2 hours. The precipitates which formed were filtered off, washed with ethanol then by diethyl ether and dried in vacuum desiccators over P_4O_{10}.

INSTRUMENTATION AND MEASURMENTS
The complexes were analyzed for C, H and N at the Micro analytical center, Cairo University, Egypt. Standard analytical methods were used to determine the copper ion content [13, 14]. Mass spectra were obtained on Shimadzu Qp-2010 plus. FT-IR spectra of the complexes were measured using KBr discs by a Bruker Alpha FT/IR 300E Fourier transform infrared spectrophotometer covering the range 400-4000 cm^{-1}, Faculty of Science, Menoufia University, Shebin El-Kom, Egypt. Electronic spectra in the 200-900 nm regions were recorded on a Perkin-Elmer 550 spectrophotometer. The thermal analysis (DTA and TGA) were carried out on a Shimadzu DT-30 thermal analyzer from room temperature to 900 ºC at a heating rate of 10 ºC/min, Faculty of Science, Menoufia University, Shebin El-Kom, Egypt. Magnetic susceptibilities were measured at 25ºC by the Gouy method using mercuric tetra thiocyanatocobaltate (II) as the magnetic susceptibility standard. Diamagnetic corrections were estimated from Pascal's constant [15]. TEM samples for colloidal suspension of the complexes in distilled water were prepared by dropping the colloids onto carbon-coated TEM grids and allowed the liquid carrier to evaporate in air then assayed by a JEOL 1400 plus transmission electron microscope [16], Faculty of Science, Alexandria University, Egypt.

INVITRO STUDIES
Mammalian cell lines
A549 cells (human lung cancer cell line) were obtained from VACSERA Tissue Culture Unit), Giza-Egypt.

Chemicals Used

Dimethyl sulfoxide (DMSO), crystal violet and trypan blue dye were purchased from Sigma (St. Louis, Mo., USA). Fetal Bovine serum, DMEM, RPMI-1640, HEPES buffer solution, L-glutamine, gentamycin and 0.25% Trypsin-EDTA were purchased from Lonza.

Crystal violet stain (1%)

It composed of 0.5% (w/v) crystal violet and 50% methanol then made up to volume with distilled H_2O and filtered through a Whatmann No.1 filter paper.

Cell line Propagation

The cells were propagated in Dulbecco's modified Eagle's medium (DMEM) supplemented with 10% heat-inactivated fetal bovine serum, 1% L-glutamine, HEPES buffer and 50µg/ml gentamycin. All cells were maintained at 37ºC in a humidified atmosphere with 5% CO_2 and were subcultured two times a week.

Cytotoxicity evaluation using viability assay

For cytotoxicity assay, the cells were seeded in 96-well plate at a cell concentration of 1×10^4 cells per well in 100µl of growth medium. Fresh medium containing different concentrations of the test sample was added after 24 h of seeding. Serial two-fold dilutions of the tested chemical compound were added to confluent cell monolayers dispensed into 96-well, flat-bottomed microtiter plates (Falcon, NJ, USA) using a multichannel pipette. The microtiter plates were incubated at 37 ºC in a humidified incubator with 5% CO_2 for a period of 24 h. Three wells were used for each concentration of the test sample. Control cells were incubated without test sample and with or without DMSO. The little percentage of DMSO present in the wells (maximal 0.1%) was found not to affect the experiment. After incubation of the cells for at 37°C, for 24 h, the viable cells yield was determined by a colorimetric method [17].

In brief, after the end of the incubation period, media were aspirated and the crystal violet solution (1%) was added to each well for at least 30 minutes. The stain was removed and the plates were rinsed using tap water until all excess stain is removed. Glacial acetic acid (30%) was then added to all wells and mixed thoroughly, and then the absorbance of the plates were measured after gently shaken on Micro plate reader (TECAN, Inc.), using a test wavelength of 490 nm. All results were corrected for background absorbance detected in wells without added stain. Treated samples were compared with the cell control in the absence of the tested compounds. All experiments were carried out in triplicate. The cell cytotoxic effect of each tested compound was calculated. The optical density was measured with the micro plate reader (SunRise, TECAN, Inc, USA) to determine the number of viable cells and the percentage of viability was calculated as [(ODt/ODc)]x100% where ODt is the mean optical density of wells treated with the tested sample and ODc is the mean optical density of untreated cells. The relation between surviving cells and drug concentration is plotted to get the survival curve of each tumor cell line after treatment with the specified compound. The 50% inhibitory concentration (IC_{50}), the concentration required to cause toxic effects in 50% of intact cells, was estimated from graphic plots of the dose response curve for each conc. using Graph pad Prism software (San Diego, CA. USA) [18].

MOLECULAR DOCKING STUDIES

Computational simulations enhanced noticeably making it feasible to utilize computational approaches in drug design. The Molecular Operating Environmental module MOE2015 software package is used to predict the biological features of candidate drugs and to anticipate the experimental results [19].

BIOLOGICAL STUDIES

Animals

50 healthy male albino rats of Wistar strain, 8 weeks old (170 - 200 g) were purchased from National Cancer Institute, Cairo, Egypt. Rats were housed in cages at regulated temperature (22- 25 °C). They were kept under good ventilation under a photoperiod of 12-h light/12-h darkness schedule with lights-on from 06:00 to 18:00. They all received a standard laboratory diet (60% ground corn meal, 10% bran, 15% ground beans, 10% corn oil, 3% casein, 1% mineral mixture and 1% vitamins mixture), purchased from Meladco Feed Company (Obour City, Cairo, Egypt) and supplied with drinking water throughout the experimental period.

Acute toxicity study

Determination of lethal dose 50 (LD_{50}) using experimental animals. The LD_{50} of the studied compound was determined as described by Akhila et al. [20]. The acute intraperitoneal toxicity of the chosen complexes was done on 20 animals (10 animals per group / 2 groups). The tested complexes were dissolved in DMSO diluted by sterile saline 0.9% NaCl in a maximum concentration of 0.2% by volume to be able to injected intra-peritoneal. The chosen complexes were administrated with graded doses of 1×10^{-6}, 5×10^{-6}, 1×10^{-5} and reached to 1×10^{-4} mmole/L/Kg body weight under the same environmental conditions. After administration of the chosen concentrations, the rats were observed for toxic effects after 24h of treatment. The toxicological effects were observed in terms of mortality and expressed as lethal dose 50 (LD_{50}). The LD_{50} for the two complexes nanoparticles were devoid of any toxicity in rats when given the selected different doses by intraperitoneal route.

EXPERIMENTAL DESIGN

Animals were allowed 10 days for adaptation. They were then randomly distributed into 3 equal groups, 10 rats each. The animal groups were recognized as follows:

1. Group 1 **(Control)**: Normal healthy animals injected intra peritoneal with 0.2% solution of DMSO dissolved in sterile 0.9% NaCl saline for 6 weeks.
2. Group 2, Complex (**1**): Each animal was injected intra peritoneal with 1×10^{-5} mmole/L of the tested complex for 6 weeks.
3. Group 3, Complex (**2**): Each animal was injected intra peritoneal with 1×10^{-5} mmole/L of the tested complex for 6 weeks.

Blood collection

At the end of the experimental period, animals were fasted overnight prior to dissection under light isoflurane anesthesia. Blood was drawn from the venacava and centrifuged at 3000g for 10 min; whole EDTA blood was collected for hematological studies.

Biochemical analyses

Liver enzymes activities, aspartate aminotransferase (AST), alanine aminotransferase (ALT) and alkaline phosphatase (ALP) were estimated using kinetic kits purchased by Human Diagnostic Kits, Germany [21]. The liver functions, albumin concentration, bilirubin (Total and direct) and kidney functions, blood urea and serum creatinine were measured using Diamond Diagnostic kits, Egypt [22]. All biochemical analyses were determined using a Biosystems BTS-310 Spectrophotometer.

Hematological analyses

Determination of hemoglobin (Hb) using Drabkin's solution [23], red blood corpuscles count (RBCs), total leucocytes count (TLC) and platelets count (PLTs) were determined manually [24].

Statistical analysis

Data were subjected to statistical significance tests using one-way analysis of variance (ANOVA), followed by Duncan's multiple range test. The statistical analysis was carried out using SPSS 20.00 software. The results were expressed as mean $\pm$ SD and the differences were considered significant at $P \leq 0.05$ [25].

RESULTS

The analytical and physical data of the metal complexes

Complex (1): Showed a yield of 72%, purple color with melting point > 300 ^{o}C.

IR: broad band centered at 3550-3352 , 3345-2875cm^{-1} which could be assigned to υ (H$_2$O), 3650- 3340, 3330-2700 cm^{-1} for υ (H-bond), 3170 cm^{-1} for υ (NH), 1290-1275 cm^{-1} for υ (C-O), 1700-1685 cm^{-1} for υ (C=O), 1665-1650 cm^{-1} for υ (C=N), 1575-830, 1550-795 cm^{-1} for υ (C= Ar), 1465-1367 cm^{-1} for υ (O-Ac), 615 cm^{-1} for υ (Cuo) and 590 cm^{-1} for υ (CuN).

Molar conductance, the molar conductivity of complex (**1**) was measured in DMSO solvent with 1.0×10^{-3}M, and showed a low magnitude of 3.5197Ω^{-1}m^{2}mol^{-1}.

Electronic spectrum (nm): λ max = 292, 315, 445, 592, 618 nm. Magnetic moment (μeff) = 1.68 B.M.

Electronic spin resonance, ESR, the spectrum of copper(II) complex (**1**) characteristic of species dα configuration having axial type of a d$_{(x2-y2)}$ ground state which is the most common for copper(II) complexes [31]. The complex showed g$_{\parallel}$ =2.0023, g$\perp$ =2.08, g$_{iso}$ = 2.13, A$_{\parallel}$ = 130G, A$\perp$ = 10 G, A$_{iso}$=50 G, G = 2.75, ΔE $_{xy}$ = 17860 cm^{-1}, ΔE $_{xz}$ = 21065 cm^{-1}, K$^2\perp$ = 1.10, K$^2_{\parallel}$ = 0.57, K^2 = 0.85, K=0.93, g$_{\parallel}$/A$_{\parallel}$ = 170.7, α^2 = 0.63, covalent β^2 = 1.8, ionic bond $\beta 1^2$ = 0.85 , covalent bond – 2B = 135, α^2_d = 55 % indicating distorted octahedral geometry around copper(II) ion.

Mass spectrum: The spectrum reveals the molecular ion peaks as follows, (m/z) at 73, 178, 355, 473 and 672 correspond to C$_5$H$_{13}$, C$_7$H$_{18}$N$_2$O$_3$, C$_{16}$H$_{25}$N$_3$O$_6$, C$_{18}$H$_{26}$N$_4$O$_7$ and C$_{21}$H$_{30}$N$_4$O$_{13}$Cu$_2$ moieties respectively.

Thermal analysis: Thermogram of complex (1) exhibited six steps decomposition, the five steps involving breaking of H-bondings accompanied with endothermic peak at 52°C. In the second step, one molecule of hydrated water was lost endothermically with appearance peak at 75 ^{o}C accompanied by 2.68% (Calcd. 2.66%) weight loss. Such a low temperature endothermic dehydrations indicated that, the water molecules were not coordinated to the metal. Then Loss of (4H$_2$O) coordinated water molecules occurred at 135°C accompanied by 11.0% (Calcd. 10.82%) weight loss. The weight loss appeared with 21.37% (Calcd. 20.97%) accompanied by an endothermic peak at 275°C was assigned to loss of two acetate groups (OAc). The endothermic peak observed at 350°C referred to the melting point of the complex. The final step observed in 410, 460, 492, 560 and 605 ^{o}C with 36.47% weight loss (Calcd. 35.95%), referred to complete decomposition of the complex which ended up with the formation of 2CuO.

Analysis calculation for $C_{21}H_{30}N_4O_{13}Cu_2$: C, 37.5; H, 4.46; N, 8.3; Cu, 18.75%. Found: C, 37.2; H, 4.356; N, 8.1; Cu, 18.53%. The molecular weight is 672.

Complex (2): Showed a yield of 75%, brownish black color with melting point > 300 °C.

IR: Broad band centered at 3560-3355 cm^{-1} which could be assigned to υ (H_2O) 3450- 3405, 1312-1290 cm^{-1} for υ (OH), 3645- 3280, 3270-2780 cm^{-1} for υ (H-bond), 3165 cm^{-1} for υ (NH), 1245-1160, 1072-680 cm^{-1} for υ (SO_4), 1725-1700 cm^{-1} for υ (C=O), 1660-1652 cm^{-1} for υ (C=N), 1570-1542, 780-755 cm^{-1} for υ (C= Ar), 620 cm^{-1} for υ (Cuo) and 592 cm^{-1} for υ (CuN).

Molar conductance: The molar conductivity of complex **(2)** was measured in DMSO solvent with 1.0×10^{-3}M, and showed a low magnitude of 7.32 $\Omega^{-1}m^2mol^{-1}$.

Electronic spectrum (nm): λ max = 290, 310, 455, 598, 607 nm. Magnetic moment (μeff) = 1.698 B.M.

Electronic spin resonance, ESR: The spectrum of copper(II) complex **(2)** characteristic of species dα configuration having axial type of a $d_{(x2-y2)}$ ground state which is the most common for copper(II) complexes [31]. The complex showed $g_{\parallel}$ =2.141, $g\perp$=2.06, g_{iso} = 2.07, $A_{\parallel}$ = 125G, $A\perp$ = 7 G, A_{iso}=50 G, G = 3.50, ΔE_{xy} = 17524 cm^{-1}, ΔE_{xz} = 21.441 cm^{-1}, $K^2\perp$ = 0.81, $K^2_{\parallel}$ = 0.52, K^2 = 0.69, K=0.82, $g_{\parallel}/A_{\parallel}$ = 192, α^2 = 0.61, covalent β^2 = 1.6, ionic bond β^2_1 = 0.83 , covalent bond – 2B = 175, α^2_d = 79 % indicating distorted octahedral geometry around copper(II) ion.

Mass spectrum: The spectrum reveals the molecular ion peaks as follows, (m/z) at 71, 201, 292, 362, 472 and 694 correspond to C_5H_{11}, $C_8H_{13}N_2O_4$, $C_{10}H_{16}N_2O_8$, $C_{12}H_{16}N_3O_{10}$, $C_{17}H_{20}N_4O_{10}S$ and $C_{17}H_{20}N_4O_{14}S_2Cu_2$ moieties respectively.

Thermal analysis: Thermogram of complex **(2)** exhibited five steps decomposition, the five steps involving breaking of H-bondings accompanied with endothermic peak at 50°C. In the second step, two molecules of hydrated water were lost endothermically with appearance peak at 78 °C accompanied by 4.92% (Calcd. 5.18%) weight loss. Such a low temperature endothermic dehydrations indicated that, the water molecules were not coordinated to the metal. The weight loss appeared with 28.89% (Calcd. 29.2%) accompanied by an endothermic peak at 270°C was assigned to loss of (2 SO_4). The endothermic peak observed at 360°C referred to the melting point of the complex. The final step observed in 400, 470, 530 and 595 °C with 33.32% weight loss (Calcd. 33.9%), referred to complete decomposition of the complex which ended up with the formation of 2CuO.

Analysis calculation: For $C_{21}H_{30}N_4O_{13}S_2Cu_2$: C, 29.4; H, 2.9; N, 8.1; Cu, 18.16%. Found: C, 29.1; H, 2.69; N, 7.87; Cu, 17.92%. The molecular weight is 694.

From all previous analyses and tests on the metal complexes, it was found that their chemical structures were as follows;
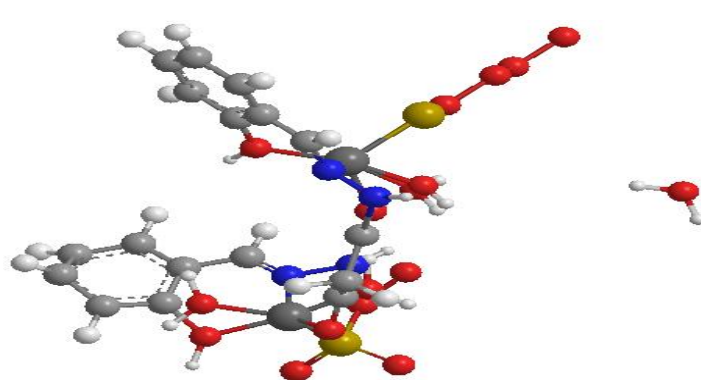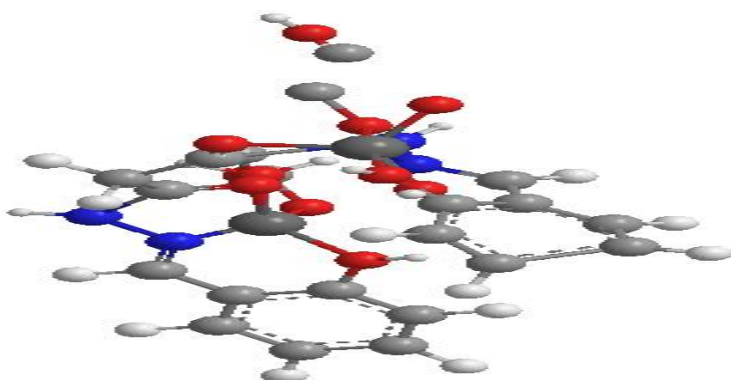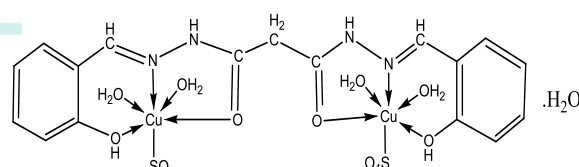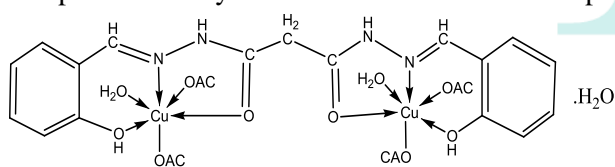

Fig. 1 Chemical and 3D structure of complex (**1**)

Fig. 2 Chemical and 3D structure of complex (**2**)

Transmission electron microscopy characterization (TEM)

The average diameter of the tested complexes particles were determined to be 26.64±7.27 nm and 24.64± 5.29 respectively as shown in **figure (3)**. The complexes particles presented in Nano size i.e., presents in a diameter between 1 and 100 nm in size that exhibit new or enhanced size-dependent properties compared with larger particles of the same material with many advantages such as: Increased bioavailability, dose. proportionality, decreased toxicity, smaller dosage form (i.e., smaller tablet), stable dosage forms of drugs which are either unstable or have unacceptably low

bioavailability in non-Nano particulate dosage forms, increased active agent surface area results in a faster dissolution of the active agent in an aqueous environment, such as the human body, faster dissolution generally equates with greater bioavailability, smaller drug doses, less toxicity and reduction in fed/fasted variability [26].
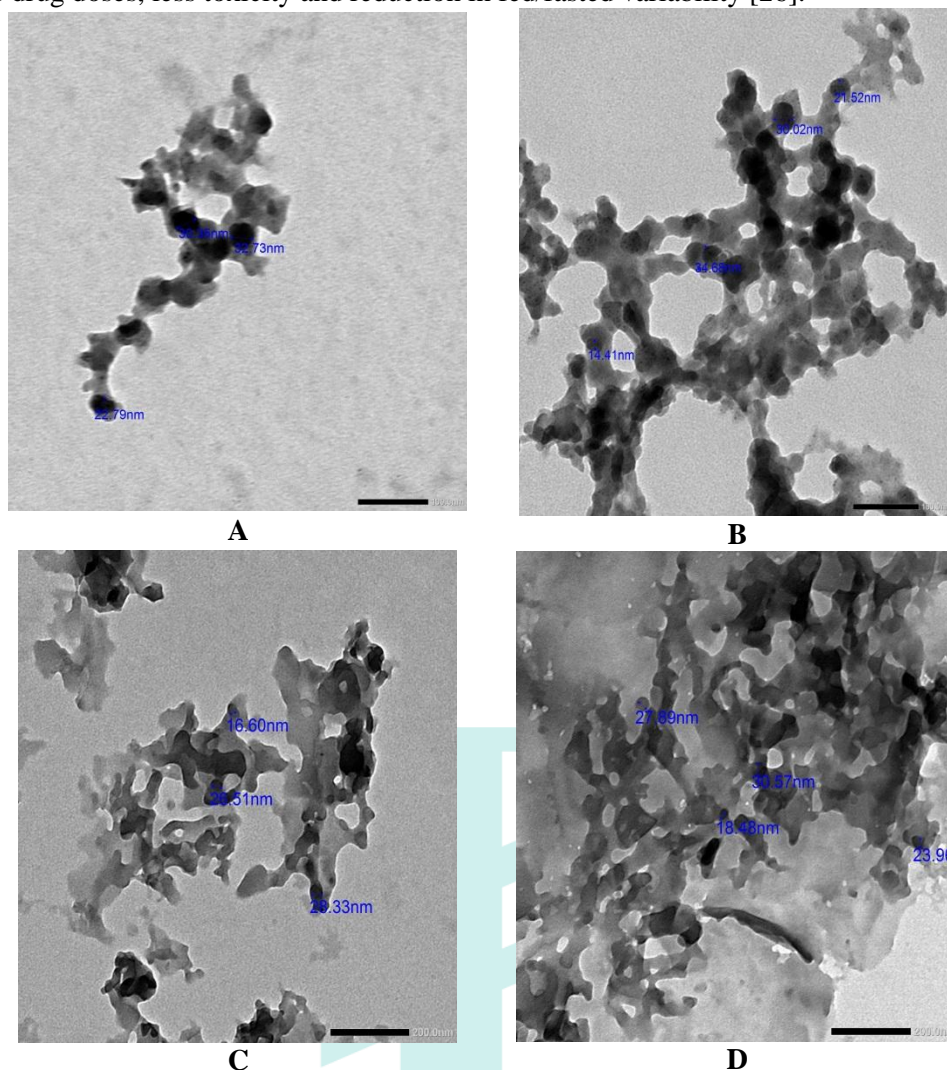

Fig. 3 [A&B] - TEM images for complex **(1)** nanoparticles [**C&D]** - TEM images for complex **(2)** nanoparticle

Evaluation of cytotoxicity against A-549 cell line

Cytotoxicity results indicated that the tested complexes NPs had IC_{50} of 3.65 ± 0.24 µg/ml for complex **(1)** and 5.02± 0.39 µg/ml for complex **(2)** demonstrated potent cytotoxicity against A549 lung cancer cell line, whereas the standard drug cisplatine had IC_{50} = 7.53± 0.51 µg/ml.

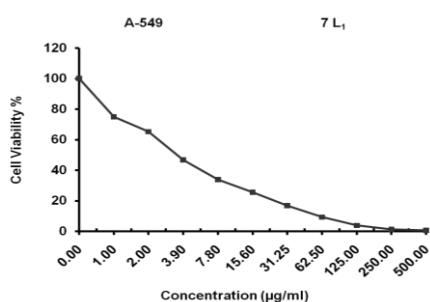**Fig. 4** Cytotoxicity of complex **(1)** against A-549 cell line
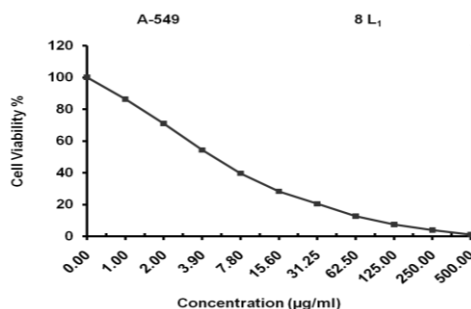
Fig. 5 Cytotoxicity of complex **(2)** against A-549 cell line
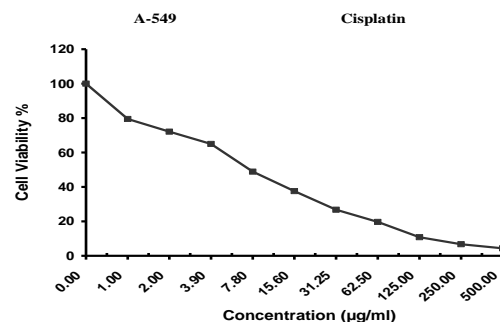
Fig. 6 Cytotoxicity of standard drug, cisplatine against A-549 cell line

The obtained data indicated the surviving fraction ratio against A549 tumor cell line increasing with the decrease of the concentration in the range of the tested concentrations. This can be explained as some metal ions bind to DNA. It seems that, changing the anion and the nature of the metal ion has effect on the biological behavior, due to alter binding ability of DNA binding, so testing of different complexes is very interesting from this point of view. Chemotherapeutic activity of the complex may be attributed to the central metal atom which was explained by Tweedy's chelation theory [27]. Also, the positive charge of the metal increases the acidity of coordinated ligand that bears protons, leading to stronger hydrogen bonds which enhance the biological activity [28]. Moreover, metal has been suggested to facilitate oxidated tissue injury through a free-radical mediated pathway analogous to the Fenton reaction [29].

Molecular docking studies

In the present study, the protein structure of 5HG5 was used as the receptors docked with the two tested complexes as inhibitors for lung cancer. Before the docking process, the preparation of the pre-protein structure was achieved by removing water molecules and adding polar hydrogen with the MMFF94x force field [30]. Docking results include ligand-receptor sites, interaction type, interaction distances (A), internal energy (E), and scoring energy (S) in kcal/mole. The negative value for energies implies the spontaneous binding of the tested inhibitor to the target protein. The data propose the best interaction stability for docked compounds. The effective ligand-receptor interaction distances were $\leq$ 3.5 A in most cases, which indicates the presence of typical real bonds and hence high binding affinity. For example, the nearest interaction is observed *via* H-donors with 5GH5 (3.08A) and complex (**1**) with scoring energy (S) -1.787 kcal/mole Further, the scoring energy function (S) is taken as an indication of high ligand-protein binding affinity based on several factors such as hydrogen bonds, deformation impact, hydrophobicity, entropy, and van der Waals interaction. Furthermore, seven binding sites were observed of different amino acids (Asp 842 and Glu 887) with complex (**1**) demonstrating their high inhibition efficacy as candidates, while the docked (copper metal complex (**2**)) Fig. 3 have effective ligand-receptor interaction distances were $\leq$ 3.5 A in most cases, which indicates the presence of typical real bonds and hence high binding affinity . For example, the nearest interaction is observed via H-donors with 5GH5 (2.99A) and complex (**1**) With scoring energy (S) -2.500 kcal Furthermore, eight binding sites were observed of different amino acids (cys 797 ,Gly 796, Leu 844,Met 793 and Met 790) with complex (**8**) demonstrating their high inhibition than copper complex (**1**).
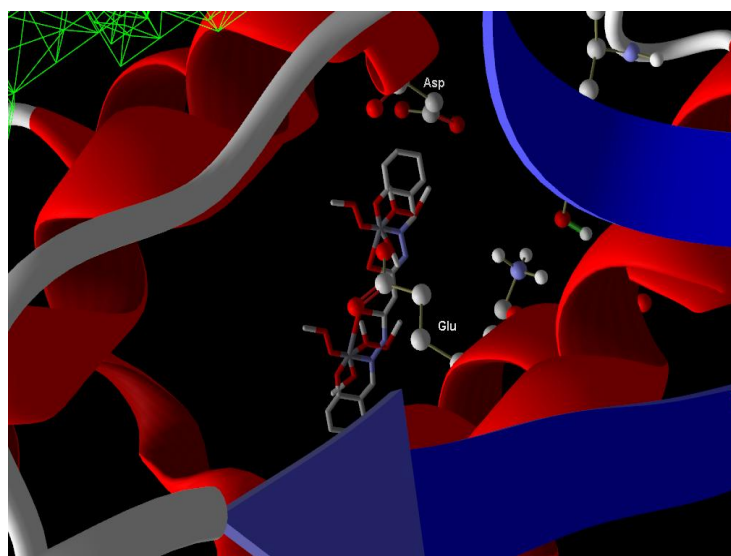

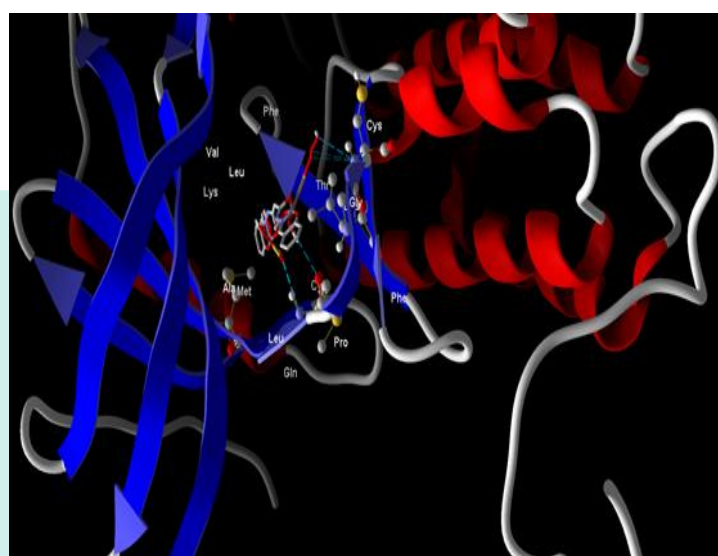**Fig. 7** Virtual molecular docking of the best docked complex (**1**) with 5GH5 protein

Fig. 8 Virtual molecular docking of the best docked complex (**2**) with 5GH5 protein

Biological studies "*Invivo* studies"
Biochemical analyses

The results of the present study [Table 1] recorded that the measurements of liver functions (AST, ALT, ALP, albumin and total bilirubin), renal functions (B.Urea & S.Creatinine) showed no significant differences between treated groups by the chosen complexes and the control group, which proves that there are no toxic side effects for the tested complexes.

Table 1 Statistical analysis (ANOVA) for liver and kidney function tests in the different groups

Parameters	Control	Complex (1)	Complex (2)
AST (U/l)	111.912±27.237	108.450±16.224	116.024 ±21.094
ALT (U/l)	36.241±9.241	34.800±4.712	35.544±7.542
ALP (U/l)	146.740±21.221	143.980±16.192	147.114±12.262
Alb (g/dl)	4.51 ±0.914	4.390 ±0.506	4.602 ±0.775
T.Bilirubin (mg/dl)	0.496±0.092	0.510±0.114	0.481±0.105
B. Urea (mg/dl)	29.331±3.092	28.897±5.227	30.004±3.719
S. Creatinine (mg/dl)	0.508 ±0.117	0.545 ±0.094	0.511 ±0.043

ANOVA: analysis of variance; **AST**: aspartate aminotransferase; **ALT**: alanine aminotransferase; **Alb**: albumin; **ALP**: alkaline phosphatase; **T. Biliribin**: Total bilirubin; each value is represented as mean ± SD**. SD**: standard deviation. Each value is represented as mean ± SD. Data with different superscripts are significantly different at $p \leq 0.05$

Hematological analysis

The results of the analysis of some hematological parameters (Hb, RBCs, TLC and platelets counts) showed no significant changes between the control group and the treated groups by the chosen complexes as follow in Table 2.

Table 2 Statistical analysis (ANOVA) for hematological tests in the different groups

Parameters	Control	Complex (1)	Complex (2)
Hb (g/dl)	15.29 ±1.547	15.102±0.87	14.982±1.148
RBCs (X 10^6/cmm)	5.764 ±0.813	5.522±0.944	5.497±0.888
TLC (X 10^3/cmm)	8.872±1.554	9.122±1.716	8.966±0.991
PLTs (X 10^3/cmm)	522.119±42.712	509.441±28.461	422.283±31.22

ANOVA: analysis of variance; **Hb**: Hemoglobin concentration; **RBCs**: Red blood corpuscles count; **TLC**: Total leucocytes count; **PLT**: Platelets count. Each value is represented as mean ± SD. **SD**: standard deviation Data with different superscripts are significantly different at $p \leq 0.05$

DISCUSSION

This study was conducted to evaluate the efficiency, the biological activity and the cytotoxic effects of two synthesized Cu (II) complexes NPs against human lung carcinoma cell line (A549 cells), *invitro* study. Results showed potent effect of Cu complex NPs more than standard drug (Cis-platin) in a dose-dependent manner, where increasing concentration of Cu complex NPs resulted in increased percentage of dead cells. This result proving that the tested complex NPs inhibit cell proliferation via induction of apoptotic cell death. In addition, Cu complex NPs produce a cytotoxic effect by reducing cell viability and causing inter-nucleosomal DNA fragmentation, G2/M cell-cycle arrest, and hypo-diploid accumulation emphasizing that the Cu complex NPs have potential anticancer properties and can be applied as cancer therapeutics.

A previous study showed that Cu complex NPs' uptake by the cells endocytosis and emphasized intracellular release of Cu^{+2} ions from Cu complex NPs (that) blocks cell division by binding to DNA causing DNA damage and contributed to the cytotoxicity and metabolic stress activating cell death via apoptosis. Also, down regulation of proliferating cell nuclear antigen, a factor critical for DNA replication and repair following Cu NP treatment, supports the anti-proliferative effects of Cu complex NPs [31]. The present biochemical and hematological results revealed that the measurements of liver functions, renal functions and different hematological parameters showed no significant differences between treated groups by the chosen complexes and the control group, which proves that there are no toxic side effects for the tested complexes.

CONCLUSION

Reports indicate that Cu complex NPs might be useful as therapeutics in cancer therapy, and Cu complex NPs in combination with Hadron therapy led to an enhancement of strongly lethal DNA damage caused by double-strand breaks. A previous study showed that Cu complex NPs uptake by the cells endocytosis and emphasized intracellular release of Cu^{2+} blocks cell division by binding to DNA causing DNA damage and contributed to the cytotoxicity and metabolic stress activating cell death via apoptosis [32]. Cu complex NPs produces a cytotoxic effect by reducing cell viability and causing inter-nucleosomal DNA fragmentation, G2/M cell-cycle arrest, and hypo-diploid accumulation emphasizing that they have potential anticancer properties and can be applied as cancer therapeutics [33]. Also, down regulation of proliferating cell nuclear antigen, a factor critical for DNA replication and repair following Cu NPs treatment, supports the anti-proliferative effects of Cu complex NPs [34]. The tested complexes NPs were thought to serve as a reservoir for metal ions that can induce DNA damage in cancer cells [35].

AUTHOR'S CONTRIBUTIONS

ASE designed the study and performed the complexes synthesis. AMA and SMA performed most of the experiments (Biochemical and hematological analyses), analyzed and interpreted the data. SAK performed and interpreted the molecular docking studies. AMA, ASE and SMA wrote the first version of the manuscript. All authors reviewed and approved the final version of the manuscript.

CONFLICT OF INTEREST

The authors have declared no conflict of interest.

FUNDINGS

The author(s) received no financial support for the research or authorship.

ETHICS APPROVAL

This study was performed after getting permission from the Institutional Animal Ethical Committee, Menoufia University, Egypt (approval ID: MUFS/S/BIO/8/23).

REFERENCES

1. Prakash, D., Venkataramanan, S. K., Gopal, G., Muralidar, S., & Ambi, S. V. (2023). Synbiotics in Lung Cancer. In *Synbiotics for the Management of Cancer* (pp. 191-204). Singapore: Springer Nature Singapore.
2. Sung, H., Ferlay, J., Siegel, R. L., Laversanne, M., Soerjomataram, I., Jemal, A., & Bray, F. (2021). Global cancer statistics 2020: GLOBOCAN estimates of incidence and mortality worldwide for 36 cancers in 185 countries. *CA: a cancer journal for clinicians*, *71*(3), 209-249.

3. Bai, X. G., Zheng, Y., & Qi, J. (2022). Advances in thiosemicarbazone metal complexes as anti-lung cancer agents. *Frontiers in Pharmacology*, *13*, 1018951.

4. Valente, A., Podolski-Renić, A., Poetsch, I., Filipović, N., López, Ó., Turel, I., & Heffeter, P. (2021). Metal-and metalloid-based compounds to target and reverse cancer multidrug resistance. *Drug Resistance Updates*, *58*, 100778.

5. Valente, A., Podolski-Renić, A., Poetsch, I., Filipović, N., López, Ó., Turel, I., & Heffeter, P. (2021). Metal-and metalloid-based compounds to target and reverse cancer multidrug resistance. *Drug Resistance Updates*, *58*, 100778.

6. Naskar, A., & Kim, K. S. (2022). Photo-stimuli-responsive cus nanomaterials as cutting-edge platform materials for antibacterial applications. *Pharmaceutics*, *14*(11), 2343.

7. Abdou, S., Abd-El Wahed, M. M., Ashour, A. M., Abu-Setta, M. H., Hassanein, O. H., & Saad, A. A. (2019). Metallo-organic Copper (II) Complex in Nano Size as a New Smart Therapeutic Bomb for Hepatocellular Carcinoma. *Journal of Chemistry and Chemical Sciences*, *9*(1), 33-44.

8. Tchounwou, P. B., Dasari, S., Noubissi, F. K., Ray, P., & Kumar, S. (2021). Advances in our understanding of the molecular mechanisms of action of cisplatin in cancer therapy. *Journal of experimental pharmacology*, 303-328.

9. El-Tabl, A.S., Abd-El Wahed, M. M., Abu-Setta, M.H.H., El-Mahsarawy, A.I., & Ashour, A.M (2022). Cytotoxicity and antitumor activity of organometallic copper (II) Nano particles in a chemically induced hepatocellular carcinoma rat model. *International Journal of Pharmaceutical Sciences and Research*, Vol.14 (3): 1000-11

10. Dutt, Y., Pandey, R. P., Dutt, M., Gupta, A., Vibhuti, A., Vidic, J., ... & Priyadarshini, A. (2023). Therapeutic applications of nanobiotechnology. *Journal of Nanobiotechnology*, *21*(1), 1-32.

11. Uzair, B., Liaqat, A., Iqbal, H., Menaa, B., Razzaq, A., Thiripuranathar, G., ... & Menaa, F. (2020). Green and cost-effective synthesis of metallic nanoparticles by algae: Safe methods for translational medicine. *Bioengineering*, *7*(4), 129.

12. Abdou, S., Abd-El Wahed, M. M., Ashour, A. M., Abu-Setta, M. H., Hassanein, O. H., & Saad, A. A. (2019). Metallo-organic Copper (II) Complex in Nano Size as a New Smart Therapeutic Bomb for Hepatocellular Carcinoma. *Journal of Chemistry and Chemical Sciences*, *9*(1), 33-44.

13. Hosny, S., Gouda, G. A., & Abu-El-Wafa, S. M. (2022). Novel nano copper complexes of a new Schiff base: green synthesis, a new series of solid Cr (II), Co (II), Cu (II), Pd (II) and Cd (II) chelates, characterization, DFT, DNA, antitumor and molecular docking studies. *Applied Organometallic Chemistry*, *36*(5), e6627.

14. Mahmoud, N. F., Fouad, O. A., Ali, A. E., & Mohamed, G. G. (2021). Potentiometric determination of the Al (III) ion in polluted water and pharmaceutical samples by a novel mesoporous copper metal–organic framework-modified carbon paste electrode. *Industrial & Engineering Chemistry Research*, *60*(6), 2374-2387.

15. Alhakimi, A. N., Almuhanna, T. A., Alnawmasi, J. S., Saeed, S., & Alhamzi, E. H. L. (2022). Synthesis, Spectroscopic Characterization, and Anticancer Activity of Metal Complexes with a Novel Schiff Base Ligand from β-Diketone Derivatives. *Journal of The Chemical Society of Pakistan*, *44*(6).

16. Mishra, N., Pal, S., Sharma, M., Nisha, R., Pal, R. R., Singh, P., ... & Saraf, S. A. (2023). Crosslinked and PEGylated Pectin Chitosan nanoparticles for delivery of Phytic acid to colon. *International Journal of Pharmaceutics*, *639*, 122937.

17. Kamiloglu, S., Sari, G., Ozdal, T., & Capanoglu, E. (2020). Guidelines for cell viability assays. *Food Frontiers*, *1*(3), 332-349.

18. El-Apasery, M. A., Abdellatif, M. E., Yassin, F. A., & Ahmed, S. M. (2023). Synthesis of Novel Disperse Dyes based on Arylazophenols: Part 2. Anticancer Activities. *Egyptian Journal of Chemistry*, *66*(4), 49-53.

19. Masoud, M. S., Yacout, G. A., Abd-El-Khalek, B. A., & Ramadan, A. M. (2023). Synthesis, Physicochemical Characterization, Biological Assessment, and Molecular Docking Study of Some Metal Complexes of Alloxan and Ninhydrin as Alterdentate Ligands. *Journal of Inorganic and Organometallic Polymers and Materials*, 1-18.

20. Arya, J., & Bist, R. (2022). The diverse ways to determine experimental dose in animals. *Hos Pal Med Int Jnl*, *5*(2), 21-24.

21. Kathak, R. R., Sumon, A. H., Molla, N. H., Hasan, M., Miah, R., Tuba, H. R., ... & Ali, N. (2022). The association between elevated lipid profile and liver enzymes: a study on Bangladeshi adults. *Scientific Reports*, *12*(1), 1711.

22. Bishr, N. M., Abdel-Rahman, A. A. H., Ashour, A. M., & Ibrahim, H. M. (2020). Biochemical effects of Toxoplasma gondii and Neospora caninium infection on diary bovine models in Menoufia Province, Egypt. *Adv. Anim. Vet. Sci*, *9*(3), 379-386.

23. Garcia-Casal, M. N., Dary, O., Jefferds, M. E., & Pasricha, S. R. (2023). Diagnosing anemia: Challenges selecting methods, addressing underlying causes, and implementing actions at the public health level. *Annals of the New York Academy of Sciences*, *1524*(1), 37-50.

24. Khan, M. I., Yasmeen Bibi, B. A., Haseeb, A., Khan, Y., Ullah, K., & Khan, S. (2022). Comparison of hematological profile changes in pre-and post-chemotherapy treatment of cancer patients. *Pakistan Journal of Medical & Health Sciences*, *16*(10), 616-616.

25. West, B. T., Welch, K. B., & Galecki, A. T. (2022). *Linear mixed models: a practical guide using statistical software*. Crc Press.

26. Mousa, S. A., Bawa, R., & Audette, G. F. (Eds.). (2020). *The road from nanomedicine to precision medicine*. CRC Press.

27. Shekhar, S., Khan, A. M., Sharma, S., Sharma, B., & Sarkar, A. (2022). Schiff base metallodrugs in antimicrobial and anticancer chemotherapy applications: a comprehensive review. *Emergent Materials*, *5*(2), 279-293.

28. Henwood, A. F., Hegarty, I. N., McCarney, E. P., Lovitt, J. I., Donohoe, S., & Gunnlaugsson, T. (2021). Recent advances in the development of the btp motif: A versatile terdentate coordination ligand for applications in supramolecular self-assembly, cation and anion recognition chemistries. *Coordination Chemistry Reviews*, *449*, 214206.

29. Singh, N., & Bhatla, S. C. (2022). Heme oxygenase-nitric oxide crosstalk-mediated iron homeostasis in plants under oxidative stress. *Free Radical Biology and Medicine*, *182*, 192-205.

30. Khelfaoui, H., Harkati, D., Saleh, B. A., Hewitt, N. L., Alnajjar, R., & El-Hiti, G. A. (2023). In-Silico Evaluation, Chemical Reactivity, and Covalent Docking Study of Various Quinazolines and Pyridopyrimidines as Inhibitors for the Epidermal Growth Factor Receptor. *Polycyclic Aromatic Compounds*, 1-26.

31. Bharathi, D., Ranjithkumar, R., Chandarshekar, B., & Bhuvaneshwari, V. (2019). Bio-inspired synthesis of chitosan/copper oxide nanocomposite using rutin and their anti-proliferative activity in human lung cancer cells. *International Journal of Biological Macromolecules*, *141*, 476-483.

32. Sajjad, H., Sajjad, A., Haya, R. T., Khan, M. M., & Zia, M. (2023). Copper oxide nanoparticles: In vitro and in vivo toxicity, mechanisms of action and factors influencing their toxicology. *Comparative Biochemistry and Physiology Part C: Toxicology & Pharmacology*, 109682.

33. Chakraborty, A., Das, A., Raha, S., & Barui, A. (2020). Size-dependent apoptotic activity of gold nanoparticles on osteosarcoma cells correlated with SERS signal. *Journal of Photochemistry and Photobiology B: Biology*, *203*, 111778.

34. Virk, P., Awad, M. A., Alanazi, M. M., Hendi, A. A., Elobeid, M., Ortashi, K. M., ... & Aouaini, F. (2023). Putative anti-proliferative effect of Indian mustard (Brassica juncea) seed and its nano-formulation. *Green Processing and Synthesis*, *12*(1), 20228119.

35. Shen, F., Fang, Y., Wu, Y., Zhou, M., Shen, J., & Fan, X. (2023). Metal ions and nanometallic materials in antitumor immunity: Function, application, and perspective. *Journal of Nanobiotechnology*, *21*(1), 20.